Results in Physics 5 (2015) 264–272

Contents lists available at ScienceDirect

Results in Physics

journal homepage: www.journals.elsevier.com/results-in-physics

Sodium enrichment on glass surface during heating of heavy-metal-containing glasses under a reductive atmosphere

Takashi Okada *, Fumihiro Nishimura, Susumu Yonezawa

Headquarters for Innovative Society-Academic Cooperation, University of Fukui, Bunkyo 3-9-1, Fukui 910-8507, Japan

ARTICLE INFO

Article history:
Received 13 August 2015
Accepted 28 September 2015
Available online 9 October 2015

Keywords:
Sodium enrichment
Heavy metal
Glass
Phase separation
Redox behavior

ABSTRACT

Sodium enrichment occurs on the surface of the glass that is in contact with the gas phase during the heat treatment of lead-containing glass under a reductive atmosphere. This technique was previously found to promote lead recovery in waste-glass treatment, and may be potentially applied to glasses containing other heavy metal oxides. Thus, the efficiencies of sodium enrichment were compared among glasses with different heavy metal species (PbO, CuO, and ZnO) in the heat-treatment under a CO-containing atmosphere. The sodium enrichment efficiencies in the treatment of the PbO- and CuO-containing glasses were higher than that in the treatment of the ZnO containing glass. This was because the efficiencies were related to the reduction of the heavy metal oxides. The mass ratio of Na to Si on the glass surface increased as the PbO concentration decreased via reduction of PbO. The sodium-rich phase was separated together with a copper-concentrated phase that was generated via the reduction of CuO. However, ZnO in the glass is thermodynamically more difficult to reduce in the CO-containing atmosphere used in the study, resulting in the lower efficiency of the sodium enrichment.

Introduction

Used electronic substrates, cathode ray tube (CRT) funnel glass, and automobile shredded dusts are regarded as hazardous wastes due to the toxicity of the heavy metals they contain. Such heavy-metal-containing wastes are also valuable resources, and the recovery of the heavy metals from them is important for both environmental protection and resource conservation. In Japan, smelting furnaces have been used for the recovery of heavy metals from electronic wastes [1], and municipal solid waste (MSW) melting processes can also be applied for metal recovery [2]. For more efficient metal recovery, however, it is necessary to develop a specific melting technique.

In melting processes, heavy metals are recovered as chlorides with high volatility. When waste materials are melted with chlorination agents, the heavy metals in the wastes are chlorinated and volatilized. The vapors of the heavy metal chlorides are then condensed in a cooling process, and the solid heavy metal chlorides are recovered. For instance, lead-containing glass is melted with $CaCl_2$ at 1000 °C to generate lead chlorides that are volatilized from the glass [3]. In the ash-melting process used by MSW facilities, the incineration bottom ash is melted with the incineration fly ash, which is a Cl-rich material, in order to promote the chlorination and volatilization of heavy metals [4,5]. However, this chlorination process causes corrosion of the melting furnace by the chlorine gas that is generated when large quantities of chlorination agents are fed into the furnace. Moreover, the recovered heavy metal chlorides must be converted to a metallic state in order to use the metal, which complicates the entire treatment process. For these reasons, it is desirable to recover heavy metals directly from waste materials in the metallic state. In the reduction-melting process, waste materials containing heavy metal oxides are melted under a reductive atmosphere, and the heavy metal oxides are reduced to their metallic states and are then separated from their oxide phases. Notably, this process does not require chlorination agents that lead to chlorine corrosion. Therefore, the reduction-melting process is preferable for the treatment of heavy-metal-containing wastes.

One of the heavy-metal-containing wastes that has attracted attention recently is CRT funnel glass, which has a considerable quantity of PbO [6]. Due to the decreasing demand for CRT televisions, closed-loop recycling (i.e., conversion of waste CRTs to new CRTs) is becoming difficult. It is necessary, therefore, to develop a new recycling technique involving lead recovery, and a variety of lead recovery processes have been proposed [7–14]. We previously studied the reduction-melting of lead-containing funnel glass under a CO-containing reductive atmosphere [12]. In our proposed

* Corresponding author. Tel.: +81 776 27 9756; fax: +81 776 27 8955.
E-mail address: t-okada@u-fukui.ac.jp (T. Okada).

http://dx.doi.org/10.1016/j.rinp.2015.09.005
2211-3797/

Table 1
Batching composition of test samples used for preparation of simulated glass.

Simulated glass	Chemical compounds (g)				
	Na_2CO_3	SiO_2	PbO	CuO	ZnO
Na_2O–SiO_2–PbO system	5.0	5.0	5.0	0	0
Na_2O–SiO_2–CuO system	5.0	5.0	0	2.5	0
Na_2O–SiO_2–ZnO system	5.0	5.0	0	0	2.5

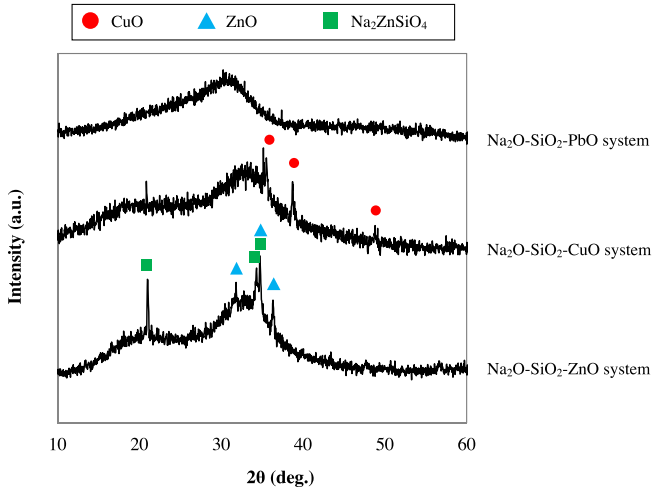

Fig. 1. XRD patterns of the simulated glass.

method, a large quantity of Na_2CO_3 was melted with the funnel glass as a flux to decrease the viscosity of the glass and promote aggregation of the generated metallic lead. However, a part of PbO remained in the residual oxide phase and the concentration

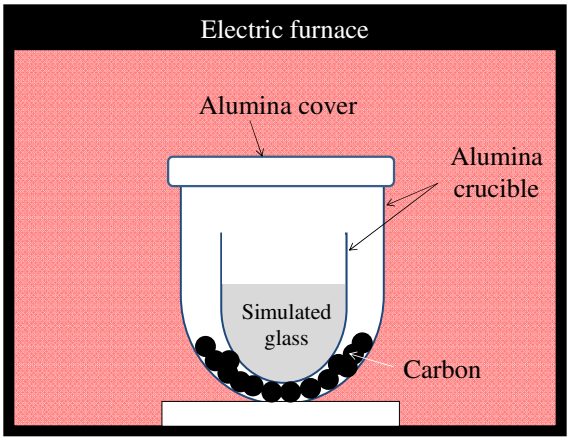

Fig. 2. Schematic of reductive heat treatment setup.

of the remaining PbO was about 2.0 wt%. To promote the lead recovery, we combined a sodium enrichment technique with the reduction-melting process [14]. After the reduction-melting at 1000 °C, the molten glass was annealed at 700 °C and the sodium oxides were concentrated on the surface of the glass that was in contact with the gas phase (referred to as the "contact surface"). The phase separated sodium oxides were extracted with water. By this water treatment, the remaining oxide phase was microparticulated and porous structures formed on the oxide surfaces. This increases surface area of the oxides and recovery of the remaining lead from the oxides in a subsequent acid leaching was promoted. Therefore, in the phase separation process, the sodium enrichment efficiency that can affect the microparticulation and porous structure of the residual oxide phase is important for heavy metal recovery in leaching processes of the oxide phase.

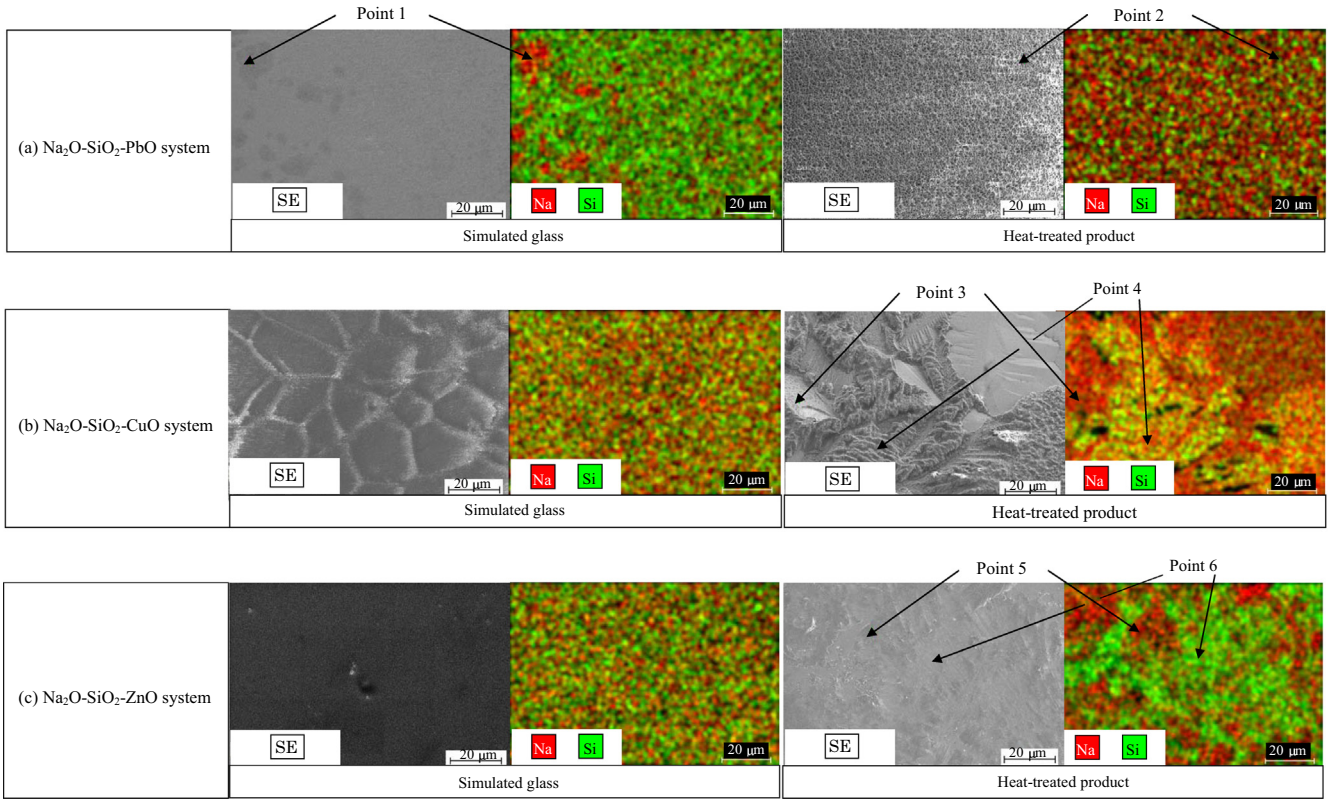

Fig. 3. Secondary electron images and mapping images of Na and Si on the contact surfaces of the simulated glass and heat-treated product (accelerating voltage in SEM observation and EDS analysis: 5 kV).

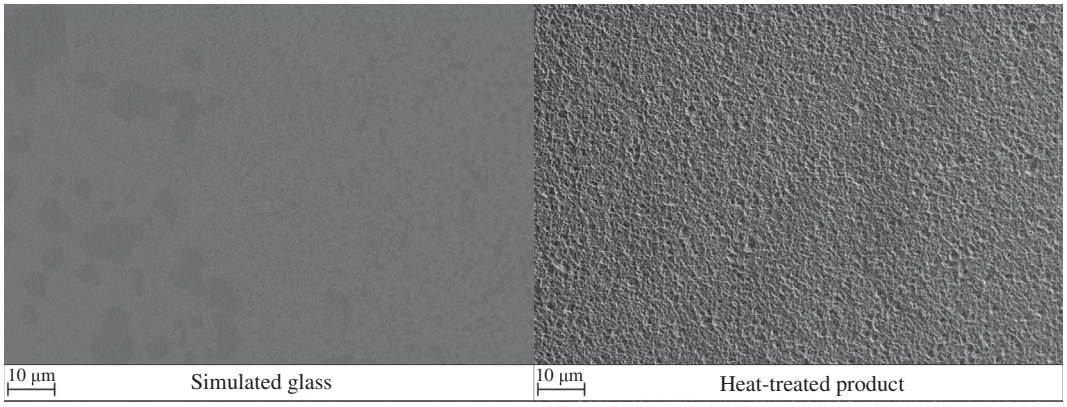

(a) Comparison between the simulated glass and heat-treated product

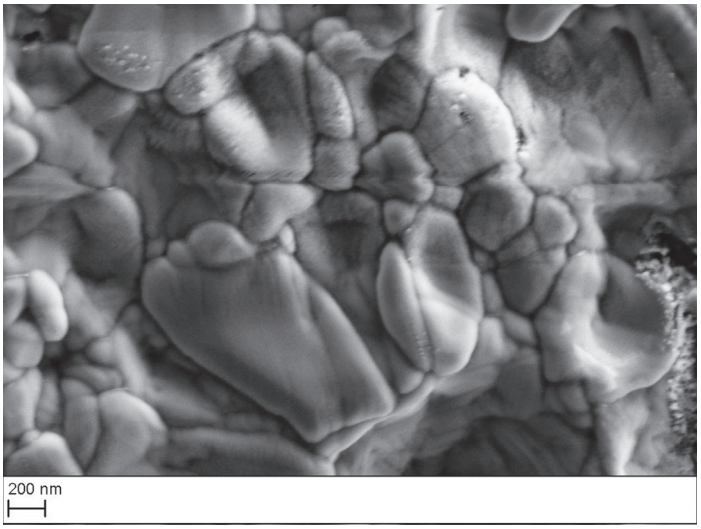

(b) Observation of the heat-treated product at higher magnification

Fig. 4. Secondary electron images of the contact surface of the simulated glass and heat-treated product in Na_2O–SiO_2–PbO system (accelerating voltage in SEM observation: 2 kV).

The phase separation of sodium in glass has been reported [15,16]. To the best of our knowledge, sodium enrichment under a reductive atmosphere during the reduction-melting process for heavy-metal-containing wastes has not yet been mechanistically investigated. During the melting process, the heavy metal oxides incorporated into the SiO_2 network of the glass are reduced to the metallic state and removed from the network. Depending on concentrations of heavy metal oxides in glass, the glass structure and electron density of SiO_2 unit in glass are different [17,18]. Removal of the heavy metals during melting results in a continual change of the glass structure and charge balance in the SiO_2 network with time. In addition, structure of glass prepared in a reductive atmosphere would be different from that of glass prepared in an oxidative atmosphere based on following authors' previous study. X-ray photoelectron spectroscopy was performed on glasses prepared under atmospheres with different oxidizing powers [19]. In the O1s and Si2p spectra, the peak positions and shapes were different for the various glass materials, even though their chemical compositions were not significantly different. For these reasons, in a reductive environment, it is possible that the sodium enrichment efficiency would be affected by the change of the structure and charge balance resulting from the reduction of the heavy metal oxides, because the phase separation is promoted by coulombic repulsions between network-modifier cations [20]. In fact, the authors previously found that such sodium enrichment was observed in a reductive atmosphere but not in an oxidative atmosphere [13]. Based on these findings, the sodium enrichment technique may be potentially applied to glasses with other heavy metal species. However, in our previous studies, the sodium enrichment has been studied on lead-containing glass but not other heavy-metal-containing glass. Depending on the heavy metal species, their redox behaviors are different and these may affect the sodium enrichment efficiencies.

In the present study, sodium enrichment during the heat treatment of heavy-metal-containing glasses under a reductive atmosphere was investigated with the purpose of comparing the sodium enrichment efficiencies between the glasses with different heavy metal species. Simulated glasses containing different heavy metal oxides were prepared using standard reagents, and each glass was heated in an electric furnace under a reductive atmosphere. The contact surfaces of the obtained materials were observed, and the sodium enrichment efficiencies were determined.

Materials and methods

Preparation of test samples

Mixtures of reagent-grade SiO_2, Na_2CO_3, PbO, CuO, and/or ZnO (Wako Chemical Co. Ltd., Osaka, Japan) were used to prepare test

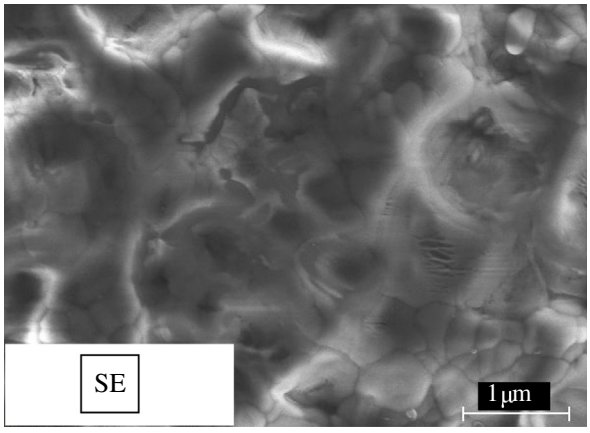

(a) Secondary electron image

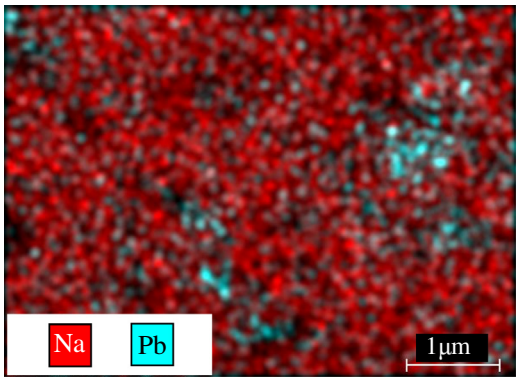

(b) Mapping image of Na and Pb

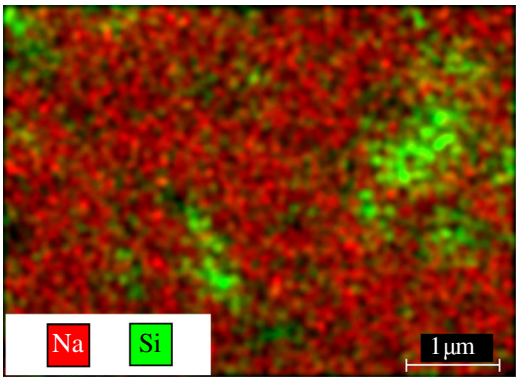

(c) Mapping image of Na and Si

Fig. 5. Secondary electron image and mapping images of Na, Pb, and Si on the contact surface of the heat-treated product in Na_2O–SiO_2–PbO system (accelerating voltage in SEM observation and EDS analysis: 5 kV).

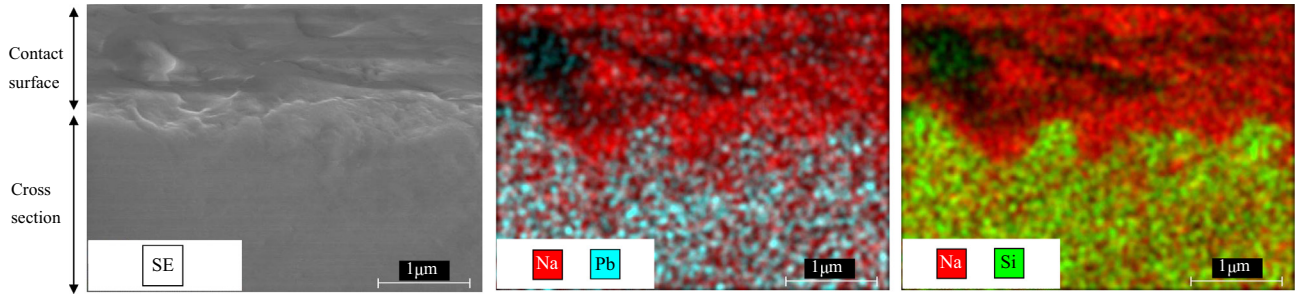

(a) Secondary electron image (b) Mapping image of Na and Pb (c) Mapping image of Na and Si

Fig. 6. Secondary electron image and mapping images of Na, Pb, and Si on the cross-section of the heat-treated product in Na_2O–SiO_2–PbO system (accelerating voltage in SEM observation and EDS analysis: 5 kV).

samples. Table 1 shows the batching compositions of the mixtures. The mixture of reagents was placed in a 30 mL alumina crucible, which was then placed in an electric furnace. The temperature in the furnace was elevated to 1000 °C over a period of 30 min, and the mixture was melted for 2 h at this temperature under atmospheric condition. The crucible was then removed from the furnace using fire tongs, and the glass melt in the crucible was allowed to cool naturally and rapidly at room temperature. This material is the test sample and referred to as "simulated glass".

Fig. 1 shows the X-ray diffraction (XRD) patterns of the simulated glasses from XRD analysis explained in Section 2.3. Broad diffraction peaks indicating the presence of amorphous phases are observed for the Na_2O–SiO_2–PbO system. Conversely, a peak for CuO is present in addition to the broad peak in the XRD pattern for the Na_2O–SiO_2–CuO system. Peaks for ZnO and Na_2ZnSiO_4 also coexist with the broad peak in the XRD pattern for the Na_2O–SiO_2–ZnO system. From the obtained XRD pattern, the crystallinity of the simulated glass was calculated as follows with the equation:

$$\text{Crystallinity}(\%) = (A_c/(A_c + A_a)) \times 100 \quad (1)$$

where A_c is the area of sharp diffraction peak corresponding to crystalline in the XRD pattern, and A_a is that of the broad diffraction peak corresponding to amorphous.

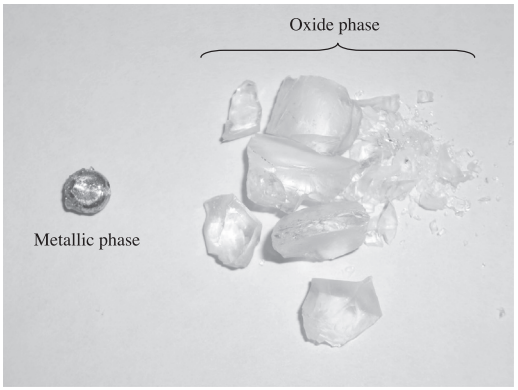

(a) Photograph

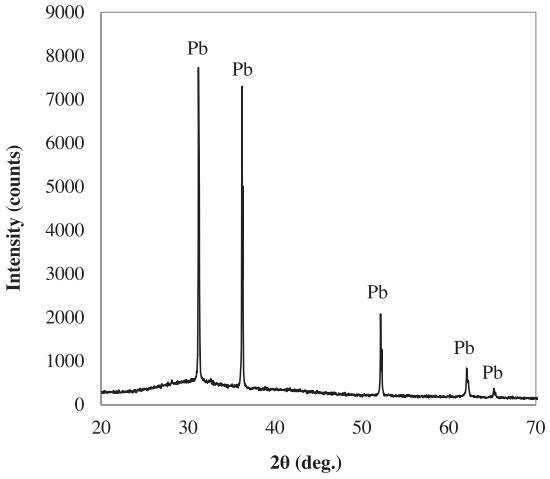

(b) XRD pattern

Fig. 7. Photograph of the heat-treated product in Na_2O–SiO_2–PbO system and XRD pattern of the metallic phase in the product.

The degree of crystallinity was 2.1% for the Na_2O–SiO_2–CuO system and 2.7% for the Na_2O–SiO_2–ZnO system, and the percentage of the amorphous phase was confirmed to be greater than that of the crystalline phase in both materials. In Fig. 1, the shapes of the broad diffraction peaks were different among the simulated glasses, implying that the structure of the glasses were also different. It is difficult to evaluate only effects of the redox behaviors of the heavy metal oxides on the sodium enrichment efficiency, separately from the effect of the structural difference. However, the discussion of the effects of the redox behaviors is meaningful

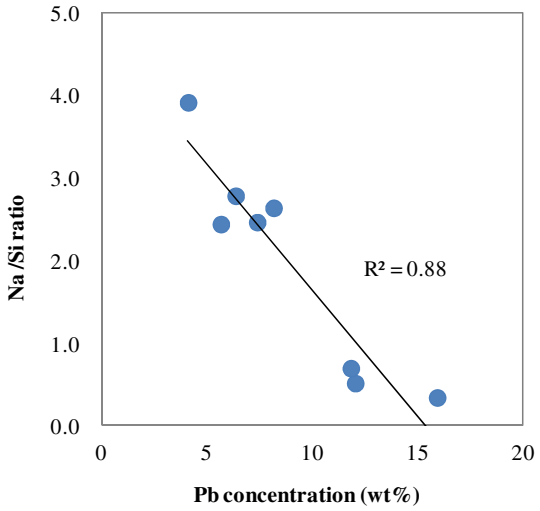

Fig. 8. Relationship between Na/Si ratio and Pb concentration on the contact surface of the heat-treated product in the Na_2O–SiO_2–PbO system.

because the sodium enrichment efficiency was related to the reduction of the heavy metals (see Section 3.1).

As explained above, the simulated glasses were prepared in an alumina crucible, and during the melting process, it is possible that a portion of the alumina in the crucible dissolved in the glasses. Therefore, to confirm the quantities of alumina in the simulated glasses, the mass ratios of alumina to silica in the simulated glasses were determined via X-ray fluorescence (XRF) analysis explained in Section 2.3. The ratios were found to be in the range from 0.0089 to 0.030 that were lower than those of the heavy metal oxides to silica in the simulated glass (0.5–1). Therefore, the effect of the alumina contamination on the sodium enrichment may be smaller than those of the heavy metal oxides.

Reductive heat treatment of the simulated glasses

The prepared simulated glass was reheated under a reductive atmosphere to cause the sodium enrichment on the glass surface. A schematic diagram of the experimental setup is shown in Fig. 2. The crucible containing the simulated glass prepared as above was directly placed in a 100 mL alumina crucible containing activated carbon (3 g). The 100 mL crucible was then covered with an alumina cover and placed in the electric furnace. The temperature of the furnace was elevated to 1000 °C over a period of 30 min, and the simulated glass in the crucible was melted for 1 h at this temperature. Subsequently, the furnace was allowed to cool naturally to 700 °C, and the glass was then heated at this temperature

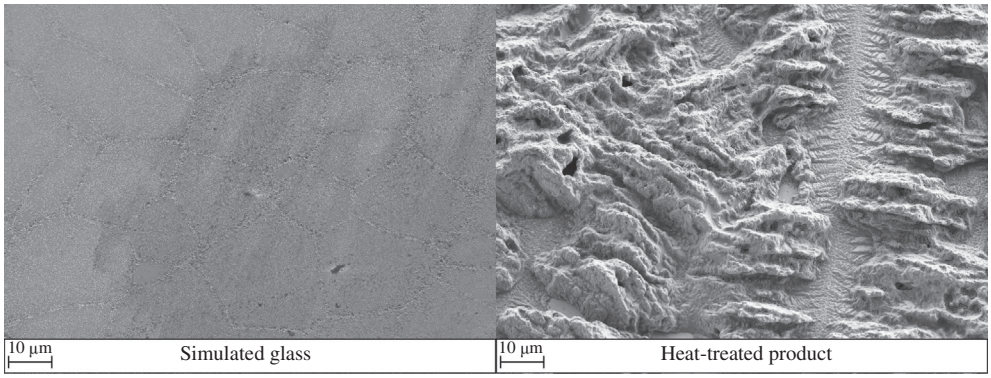

Fig. 9. Comparison of the contact surfaces between the simulated glass and heat-treated product in Na_2O–SiO_2–CuO system (accelerating voltage in SEM observation: 2 kV).

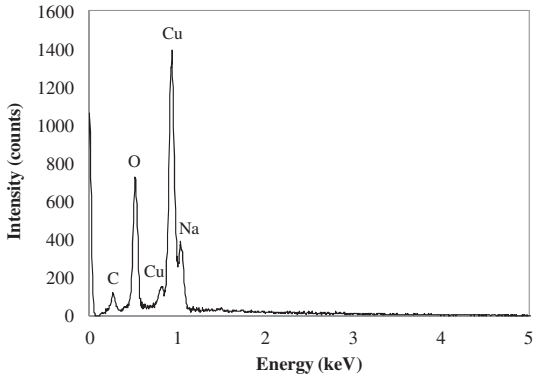

(a) Point 3 in Figure 3 (b)

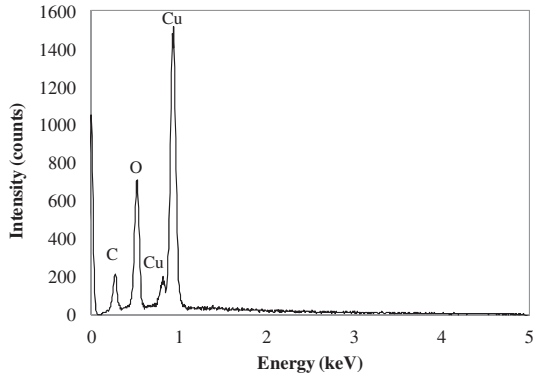

(b) Point 7 in Figure 11 (b)

Fig. 10. Spectrum of point analysis on the contact surface of the heat-treated product in Na_2O–SiO_2–CuO system (accelerating voltage in SEM observation and EDS analysis: 5 kV).

for 1 h to cause phase separation. Finally, the glass was allowed to cool naturally to room temperature. The obtained material is referred to as the "heat-treated product".

Analytical methods

The chemical composition of the simulated glass was determined via XRF analysis on a Shimadzu LAB CENTER XRF-1800 system (Shimadzu, Kyoto, Japan). In XRF, the fundamental parameter method was used for the quantification of the glass. To check the analytical error, each sample was analyzed twice repeatedly and coefficient variation of the element concentrations was 0.10–9.3%. The crystal states of the simulated glasses were evaluated via XRD analysis on a Bruker AXS D8 ADVANCE system (Bruker AXS, Kanagawa, Japan). Type of photon source was a Cu Kα source (k = 1.5406 Å). An operating voltage was 40 kV and a beam current was 40 mA. Step size was 0.035°° and scan rate was 1.5 s per step. A powder sample obtained by grinding the simulated glass was analyzed with the above condition and XRD patterns of the samples were collected between 10° and 80°. The contact surfaces of the simulated glasses and heat-treated products were observed using field-emission scanning electron microscopy (FE-SEM) on a Seiko Instruments/Zeiss ULTRA plus system (Seiko Instruments, Chiba, Japan; Zeiss Oberkochen, Germany), which was equipped with an energy-dispersive X-ray spectrometer (Bruker AXS, Kanagawa, Japan). The simulated glass and heat-treated product were crushed, and a part of the crushed piece was covered with aluminum foil to prevent static charge on the piece in the FE-SEM observation. A 1 mm square area of the covered aluminum foil was cut, and the exposed area of the piece was observed by FE-SEM. An aperture size was 30 μm, and accelerating voltage was changed from 2 kV to 5 kV.

Results and discussion

Na_2O–SiO_2–PbO system

Fig. 3 (a) shows the mapping images for Na and Si on the contact surfaces for the Na_2O–SiO_2–PbO simulated glasses and corresponding heat-treated products. After heat treatment, the area where sodium is concentrated on the surface in the Na_2O–SiO_2–PbO system expands. Point analysis using EDS was then performed on the sodium-concentrated area before and after heat treatment, and the mass ratio of Na to Si (Na/Si ratio) was determined to be 0.29 before (Point 1) and 6.1 after (Point 2) treatment. Therefore, sodium enrichment on the contact surface was promoted by heat treatment under a reductive atmosphere. On the sodium-concentrated surface, an indented structure is evident (Fig. 4 (a)), and submicron-sized fine structures are observed at higher magnification (Fig. 4 (b)).

As mentioned in Section 1, sodium enrichment may be affected by the reduction of heavy metal oxides. To clarify this relationship, therefore, the distributions of Pb, Na, and Si on the contact surface were investigated. Fig. 5 shows the mapping images for Pb, Na, and Si on the surface of the Na_2O–SiO_2–PbO heat-treated product. Most of the observed area includes the sodium-concentrated phase, and Pb and Si are also present in a portion of the area. However, the lead concentration is lower in the area of high sodium concentration. Fig. 6 shows the mapping images for the elements in a cross-section of the heat-treated product. Compared to the interior, the concentration of lead is lower in the area on the contact surface with a high sodium concentration. The lower lead concentration was caused by the reduction of PbO during heat treatment, which subsequently resulted in removal of the generated metallic lead from the glass phase. In fact, a metallic phase was generated during heat treatment of the Na_2O–SiO_2–PbO glass (Fig. 7(a)), as indicated by the appearance of a peak corresponding to metallic lead in the XRD pattern for the metallic phase (Fig. 7 (b)). If the structural change in the SiO_2 network due to the lead removal affected the sodium enrichment efficiency, the quantity of Na should be negatively correlated with that of the Pb on the contact surface of the heat-treated product. Thus, the chemical compositions of several points in the observed area in Fig. 5 were determined using EDS in order to confirm this correlation. Fig. 8 shows the relationship between the Na/Si ratio and the Pb concentration. It can be seen that the Na/Si ratio increases as the Pb concentration decreases, indicating that sodium enrichment was indeed promoted by the reduction and removal of PbO in the glass.

Na_2O–SiO_2–CuO system

In the Na_2O–SiO_2–CuO system, an indented structure is also observed on the contact surface after heat treatment (Fig. 9), and the structure is larger than that for the Na_2O–SiO_2–PbO system (Fig. 4(a)). On a pitted area in the structure, sodium enrichment is also observed (Fig. 3(b)). In this area (Point 3), silicon was not detected, as shown in Fig. 10(a) (peak position in the Si–Kα spectrum is known to be 1.739 keV). On the other hand, the Na /Si ratio determined using EDS was 0.53 on the Si-rich area (Point 4).

Also, relationship between sodium enrichment and the reduction of heavy metal oxides is discussed. Mapping images for Cu, Na, and Si on the contact surface of the Na_2O–SiO_2–CuO heat-treated product are also shown in Fig. 11. Not only is an area of

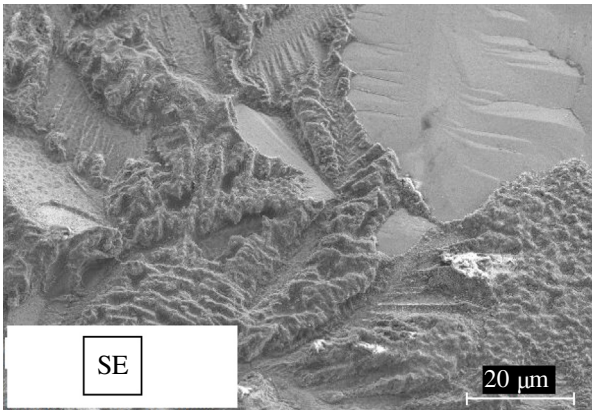

(a) Secondary electron image

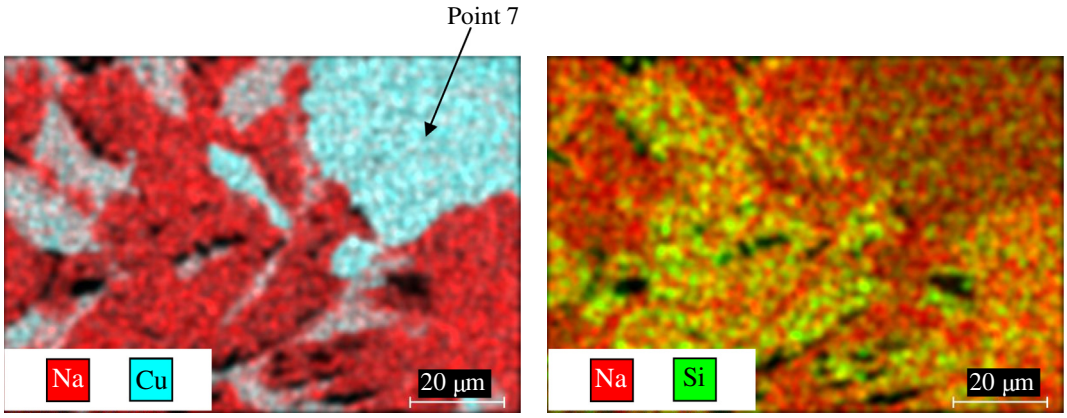

(b) Mapping image of Na and Cu

(c) Mapping image of Na and Si

Fig. 11. Secondary electron image and mapping images of Na, Cu, and Si on the contact surface of the heat-treated product in Na_2O–SiO_2–CuO system (accelerating voltage in SEM observation and EDS analysis: 5 kV).

sodium concentration evident, but an area of copper concentration that was separated from the silicon is evident as well. The results of point analysis using EDS of the copper-concentrated area (Point 7 in Fig. 11 (b)) are shown in Fig. 10 (b). Peaks corresponding to Cu, O, and C are observed, whereas no peaks for Si and Na are evident. The molar ratio of O to Cu in the area was 0.89 (<1), and the quantity of oxygen was insufficient for the formation of CuO. In addition, the molar ratio of O to Cu plus C in the area was 0.65 (<1). Assuming that the C originated from carbon dioxide contaminating the area of copper concentration, the quantity of oxygen that combined with copper was much lower than that of CuO. This implies that the CuO in the glass was possibly reduced by CO and valence of the copper became lower than +2. The phase separated copper-concentrated materials remained on the contact surface without settling, and this behavior for copper was different from that of lead in the Na_2O–SiO_2–PbO system. However, in the Na_2O–SiO_2–CuO system, the reduction of CuO is also thought to have proceeded in the area of copper concentration. Thus, if CuO reduction promoted sodium enrichment, Na and Cu would coexist on the contact surface of the heat-treated product. Fig. 12(a) shows the secondary electron image and mapping images for Cu and Na in the copper-concentrated area on the surface of the heat-treated Na_2O–SiO_2–CuO product. These images were combined to provide the image shown in Fig. 12(b). A material with a high sodium concentration is evident in the phase-separated, Cu-concentrated area. This result implies that sodium enrichment occurred together with the reduction of CuO in the glass.

Na_2O–SiO_2–ZnO system

In the mapping image for the Na_2O–SiO_2–ZnO system, an area where sodium is concentrated is also present (Fig. 3(c)). The Na/Si ratios determined using EDS were 1.8 on the Na-rich area (Point 5) and 0.75 on the Si-rich area (Point 6). However, the Na/Si ratio in the Na-rich area (Point 5) is lower than that for the Na_2O–SiO_2–PbO system (1.8 for Point 5 vs. 6.1 for Point 2). Therefore, the sodium enrichment efficiency was lower in the Na_2O–SiO_2–ZnO system than those in Na_2O–SiO_2–PbO and Na_2O–SiO_2–CuO systems. This reason is considered below.

As explained in Section 1, the structural change caused by the reduction of the heavy metal oxides in the glass should affect the sodium enrichment efficiency. As the quantity of heavy metal oxide that is reduced and removed from the glass phase increases, the structural change in the SiO_2 network becomes more dramatic. Therefore, the redox behavior of the heavy metal oxide in the glass must influence the degree of structural change and, consequently, the sodium enrichment efficiency. As an indicator of the redox behaviors of the metal oxides used in this study, Ellingham diagrams described using thermodynamic data [21] are shown in Fig. 13. The Gibbs free energies for oxidation of the heavy metals are provided. In addition, because the reductant in the present reduction-melting process was CO, the Gibbs free energy for the oxidation of CO is included for comparison. It can be seen in the figure that the Gibbs free energies for the oxidation of PbO and CuO are larger than that for the oxidation of CO at 1000 °C (1273 K),

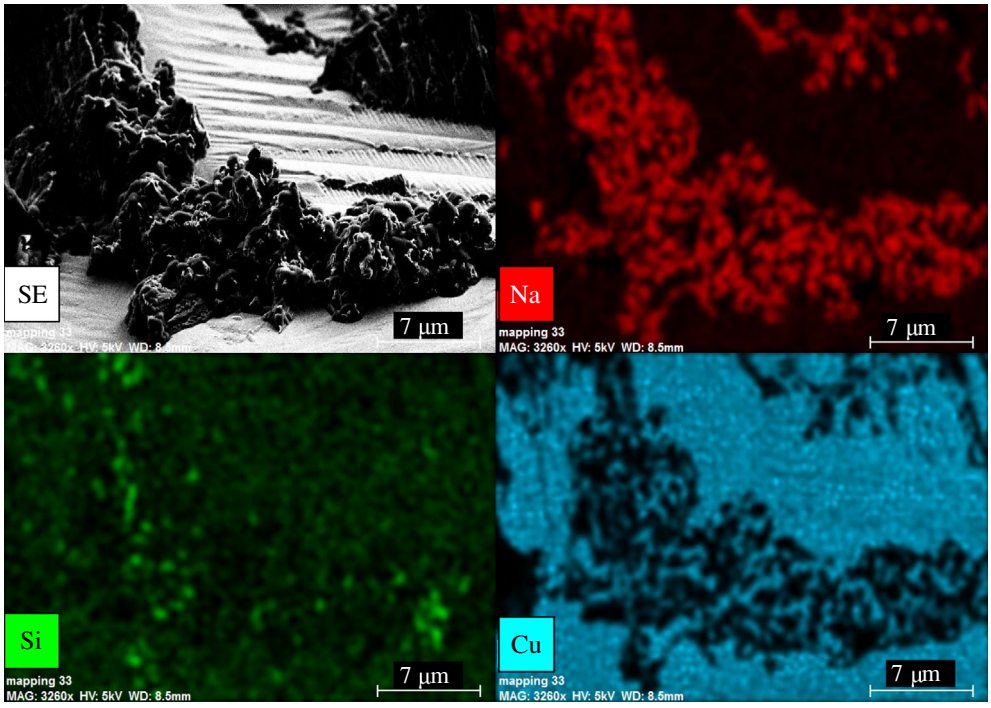

(a) Each image

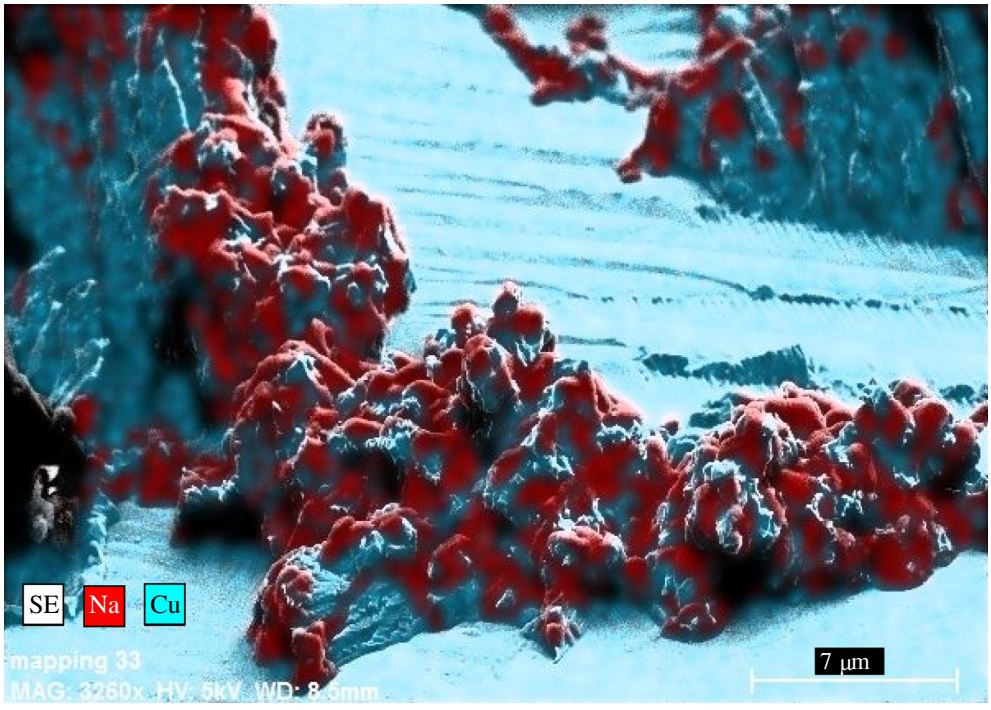

(b) Combined image

Fig. 12. Secondary electron image and mapping images of Na, Cu, and Si on the contact surface of the heat-treated product in Na_2O–SiO_2–CuO system (accelerating voltage in SEM observation and EDS analysis: 5 kV).

and thus these heavy metal oxides can be reduced by CO. As explained in Section 3.1, a metallic phase was generated during heat treatment of the Na_2O–SiO_2–PbO glass (Fig. 7(a)). Also, in the Na_2O–SiO_2–CuO system, the reduction of CuO also occurred, and the reduced copper was phase-separated from the glass phase after heat treatment (see Section 3.2). On the other hand, it can be seen in Fig. 13 that the Gibbs free energy for the oxidation of ZnO is lower than that for the oxidation of CO at 1000 °C (1273 K), and thus ZnO is thermodynamically more stable than metallic Zn under the conditions used for heat treatment in the present study. Therefore, in the Na_2O–SiO_2–ZnO system, the reduction of ZnO by CO did not occur, which resulted in a lower degree of structural change

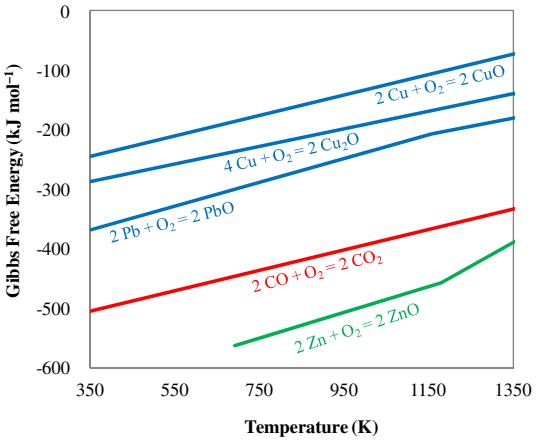

Fig. 13. Ellingham diagram.

during the heat treatment process and, consequently, a lower sodium enrichment efficiency.

Conclusion

In this study, a sodium enrichment technique was applied to the reduction-melting of heavy-metal-containing glasses. The sodium enrichment efficiencies were compared between the glasses with different heavy metal species. When glasses containing PbO and CuO, which can be reduced by CO, were heated in a reductive atmosphere, the sodium was concentrated on the surfaces of the glasses that were in contact with the gas phase. On the other hand, when the glass containing ZnO, which is more difficult to reduce with CO, was heated, the sodium enrichment efficiency was lower. Therefore, the redox behaviors of the heavy metal oxides in each glass significantly influenced the sodium enrichment efficiency.

These findings should be of great assistance for determining the appropriate conditions for efficient sodium enrichment during the reduction-melting of heavy-metal-containing wastes to promote the heavy metal recovery. This technique also enables the recovery of the sodium that is used as a flux and formation of a porous structure on the residual silica-rich oxide phase that can be used as an absorbent.

Acknowledgments

This research was supported in part by “Grants-in-Aid for Scientific Research” from the Japan Society for the Promotion of Science (Grant number: 26740041).

References

[1] Yoshida S. J Jpn Soc Waste Manage Experts 2011;22:448–52 [in Japanese].
[2] Jung CH, Osako M. Chemosphere 2007;69:279–88.
[3] Grause G, Yamamoto N, Kemeda T, Yoshioka T. Int J Environ Sci Technol 2014;11:959–66.
[4] Jung CH, Matsuto T, Tanaka N. Waste Manage 2005;25:301–10.
[5] Okada T, Tomikawa H. Waste Manage 2013;33:605–14.
[6] Méar F, Yot P, Cambon M, Ribes M. Waste Manage 2006;26:1468–76.
[7] Chen M, Zhang FS, Zhu J. J Hazard Mater 2009;161:1109–13.
[8] Sasai R, Kubo H, Kamiya M, Itoh H. Environ Sci Technol 2008;42:4159–64.
[9] Wang Y, Zhu JX. J Hazard Mater 2012;215–216:90–7.
[10] Matsumoto M, Umeda Y, Masui K, Fukushige S. In: Inano H, editor. Effect of alkali metal oxide on Pb recovery from the waste CRT glass by reduction melting method. Dordrecht, Heidelberg, New York, London: Springer; 2012. p. 896–900.
[11] Okada T, Inano H, Hiroyoshi N. J Soc Inf Display 2012;20:508–16.
[12] Okada T, Yonezawa S. Waste Manage 2013;33:1758–63.
[13] Okada T, Yonezawa S. Waste Manage 2014;34:1470–9.
[14] Okada T, Nishimura F, Yonezawa S. Waste Manage 2015 [Available online].
[15] Fujita S, Kato Y, Tomozawa M. J Non-Cryst Solids 2003;328:64–70.
[16] Wheaton BR, Clare AG. J Non-Cryst Solids 2007;353:4767–78.
[17] Wang PW, Zhang L. J Non-Cryst Solids 1996;194:129–34.
[18] Mekki A, Holland D, McConville CF. J Non-Cryst Solids 1997;215:271–82.
[19] Okada T. J Hazard Mater 2015;292:188–96.
[20] Hudon P, Baker DR. J Non-Cryst Solids 2002;303:299–345.
[21] Knacke O, Kubaschewisk O, Hesselmann K. Thermochemical properties of inorganic substances. 2nd ed. Springer-Verlag, Verlag Stahleisen; 1991.